Laser-induced phonon spectroscopy. Optical generation of ultrasonic waves and investigation of electronic excited-state interactions in solids

Keith A. Nelson, D. R. Lutz, and M. D. Fayer

Department of Chemistry, Stanford University, Stanford, California 94305

Larry Madison

Department of Physics, Stanford University, Stanford, California 94305

(Received 22 December 1980)

Crossed laser pulse excitation generates high amplitude, counterpropagating, ultrasonic waves (acoustic phonons of selected wave vector) *via* direct coupling between the optical electromagnetic field and the material acoustic field. The technique allows optical generation of ultrasonic waves, conveniently tunable to at least 20 GHz. The coupling mechanism, which does not involve optical absorption, is discussed in detail in terms of electrostriction. The periodic density changes resulting from the acoustic waves cause spectral shifts whose magnitudes reflect the strengths of excited-state intermolecular interactions and excited-state phonon interactions. The first quantitative measurements of spectral shifts by laser-induced phonon spectroscopy (LIPS) are reported. In pentacene in p-terphenyl, spectral shifts on the order of 1 cm^{-1} are measured using laser-induced phonons propagating along the b crystallographic axis. Orientation of the phonon wave vector along various crystalline directions allows investigation of the anisotropic excited-state intermolecular interactions.

I. INTRODUCTION

In solids random fluctuations in intermolecular separations, brought about by thermally occupied phonons, modulate intermolecular interactions and affect electronic excited-state dynamical processes. Exciton-phonon scattering in pure molecular crystals, for example, can determine the nature and range of excited-state transport.[1] The role of excited-state phonon interactions in excimer formation and solid-state photochemical reactions has been discussed recently.[2]

Direct measurements of excited-state intermolecular interactions in solids have been rather few. Most have taken the form of density-dependent spectroscopy in which a large hydrostatic pressure (about 1–100 kbar) is applied and spectral shifts on the order of 100 cm^{-1} are observed.[3] At pressures of many kbar the crystals are far from their normal equilibrium configurations. Typical density changes are substantial. These experiments yield valuable information about polarizabilities and other phenomena. However, the results are not directly applicable to the investigation of excited-state phonon interactions found under normal conditions. Spectral shifts arise because the ground-state and excited-state intermolecular interactions respond differently to changes in density. In most organic molecular crystals the excited state is more polarizable than the ground state, and the excited-state–ground-state energy separation decreases (the spectrum red shifts) as the density is raised. The high-pressure experiment averages over all the intermolecular interactions, and information on anisotropies is lost. This has spurred the development of new techniques for carrying out

investigations at closer-to-normal densities.[4]

Recently, a unique probe of the dynamics of excited-state intermolecular interactions in molecular crystals was reported.[5] The technique, called laser-induced phonon spectroscopy (LIPS), employs picosecond laser pulses crossed inside a sample to generate counterpropagating, high-amplitude ultrasonic waves whose wavelength and orientation are fixed by the geometry of the optical-interference pattern (see Fig. 1). The sinusoidal density variations resulting from the

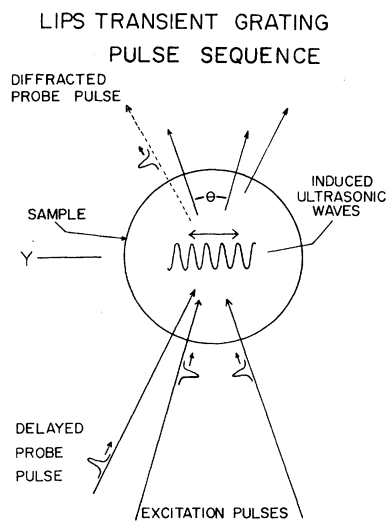LIPS TRANSIENT GRATING
PULSE SEQUENCE

FIG. 1. Schematic illustration of the LIPS transient grating experiment. The crossed excitation pulses generate counterpropagating acoustic waves (phonons) with the wavelength and orientation of the optical-interference pattern. Phonon-induced spectral shifts create a diffraction grating which Bragg-diffracts the delayed probe pulse. The phonon wavelength is given by $\Lambda = \lambda/2\sin(\theta/2)$, where λ is the excitation wavelength.

acoustic waves cause small shifts in the absorption spectrum of the material. These spectral shifts are detectable by Bragg diffraction of a probe laser pulse off of the sinusoidal optical-density transient grating pattern. Since the spectral shifts arise due to a directed, coherent ultrasonic wave (a highly occupied phonon of definite wave vector) whose orientation in the crystal is easily varied, the anisotropy of the excited-state intermolecular interactions can be investigated. The excited-state phonon interaction is directly measured for a phonon of selected wave vector at conditions close to normal density.

In this paper we report the first quantitative measurements of spectral shifts with this technique. Shifts on the order of 1 cm^{-1} are observed in pentacene in p-terphenyl crystals at room temperature. These are easily measured despite the pentacene linewidth of about 170 cm^{-1}. Results of various phonon wave-vector alignments are reported. In addition, a number of other materials are examined.

The coupling of the crossed laser pulses to the acoustic waves is also discussed in detail. Extensive experimental evidence presented in the next section shows that the excitation pulses produce an acoustic response described by

$$S_{22} = A\{\cos ky - \tfrac{1}{2}[\cos(\omega t + ky) + \cos(\omega t - ky)]\}$$
$$= A\cos ky\,(1 - \cos\omega t), \qquad (1)$$

where S_{22} is the strain component defined by

$$S_{22} = \frac{\partial u_2}{\partial y}, \qquad (2)$$

and u_2 represents displacement in the y direction. A is the acoustic wave amplitude. The phonon wave vector is fixed by the geometry of the optical-interference pattern, as shown in Fig. 1. We have assumed that only longitudinal waves are generated (generation of other types of waves is considered in Sec. III).

The instantaneous density change $\delta\rho$ at any point is given by

$$\delta\rho = -\rho_0 S_{22}, \qquad (3)$$

where ρ_0 is the normal material density. Since the strain-induced density changes give rise to spectral shifts which produce a sinusoidal optical-density pattern, a transient grating, we will refer to the phonon wave vector as the grating wave vector. The optical-interference maxima, taken in Eq. (1) to be at $y = 0$, $2\pi/k$, $4\pi/k, \ldots$, will define the transient grating (TG) peaks and the interference minima will define the grating nulls.

Examination of Eq. (1) shows that the acoustic disturbance contains two types of terms: a set

of counterpropagating waves (a standing wave) plus a time-independent, spatially sinusoidal density "offset", which is exactly cancelled by the time-dependent term once each acoustic cycle (an acoustic cycle $\tau_{ac} = 2\pi/\omega$). This disturbance causes the material density at the grating peaks to oscillate between normal and a reduced value, while the density at the grating nulls oscillates between normal and an equally increased value. The density returns to normal throughout the grating region once each acoustic cycle. This type of behavior would be expected if the effect of the picosecond laser excitation pulses were to deposit heat into the grating peaks, essentially instantaneously establishing a sinusoidal temperature distribution. The impulse response of the medium then consists of counterpropagating waves plus a static density offset as in Eq. (1).[5] The waves eventually move out of the grating region and the offset decays due to thermal diffusion. Both of these processes can be neglected on the time scale (~ 10 ns) of the observations.

In the original description of the LIPS effect,[5] it was assumed that heating of the grating peaks took place via optical absorption into high-lying vibrationally excited levels of S_1 followed by rapid radiationless relaxation. However, results of recent experiments discussed in detail in Sec. IV demonstrate that although Eq. (1) is the correct description of the acoustic disturbance, acoustic wave generation takes place independently of optical absorption. In these experiments, variation of the concentration of an absorbing species (pentacene) in a host lattice (p-terphenyl) over 2 orders of magnitude was found to have no effect on acoustic wave generation. Phonon generation was also observed when the excitation wavelength was tuned to the red side of the pentacene origin, so the initially prepared state was not vibrationally excited. Finally, LIPS experiments have been done on samples with negligible optical absorption.

These results suggest a direct coupling between the electromagnetic (em) field of the crossed laser pulses and the acoustic field of the medium. The acoustic wave amplitude shows a linear dependence on laser excitation intensity, suggesting electrostrictive coupling[6] as the appropriate mechanism. This is treated in detail in Sec. III. It is found that electrostriction does predict effective coupling between the excitation pulses and phonons of the grating wave vector, resulting in counterpropagating waves. Furthermore, the theory predicts that during the time that the laser pulses are crossing through the medium there is a static, spatially sinusoidal density offset as described above. However, current theoretical analysis predicts that the offset disappears as the pulses

leave the crystal, after which time only the counterpropagating wave remain. The experimental observations, which include times long after the excitation pulses pass through the crystal, demonstrate the continued presence of the density offset. This is discussed in detail in the next section. The discrepancy may lie in the fact that the theory of electrostriction (including the electrocaloric effect[7]) does not account for heat deposited into the system throughout the duration of the pulses. Thus some details of the mechanism of phonon generation in the LIPS experiments remain unresolved.

In the next section we discuss experimental results which verify Eq. (1) as the correct description of the acoustic disturbance. The analysis is independent of the model used to describe acoustic wave generation (optical absorption, electrostriction, etc.). It is useful to firmly establish Eq. (1) at this point so that in the subsequent theoretical discussion of the mechanism of phonon generation the experimentally demonstrated result is known. In Sec. III A, we show how spectral shifts can be quantitatively determined from LIPS transient grating data. Although optical absorption is unrelated to phonon generation, it does result in a spatially varying, sinusoidal excited-state concentration grating which can Bragg-diffract light in the same manner as the phonon-induced spectral shift grating. Thus transient grating diffracted signal arises from two superimposed gratings. From Eq. (1) it is clear that diffraction due to phonon-induced spectral shifts will be modulated at the acoustic frequency and will vanish once each acoustic cycle. Diffraction from an excited-state concentration grating decays exponentially due to the excited-state lifetime. The two effects are easily separated, and Sec. III A shows how the magnitude of the spectral shifts can be directly determined from LIPS transient grating data. In Sec. III B electrostrictive coupling between the crossed laser pulses and the acoustic field is treated in detail. In Sec. IV the experimental setup is briefly described. In Sec. V LIPS measurements of spectral shifts in pentacene in p-terphenyl are presented. Additional LIPS experiments in this and other systems which provide insight into the mechanism of phonon generation are described. In Sec. VI some applications of the LIPS technique are discussed.

The central points in the paper are the following: (1) The LIPS technique allows convenient optical generation of high-amplitude ultrasonic waves in a wide variety of condensed media, continuously tunable up to at least 20 GHz. (2) The technique is employed to perform a new type of density-dependent spectroscopy in which measurements are made at near-normal densities. This can provide information about electronic excitation interactions and excited-state phonon coupling. The first quantitative LIPS measurements are reported. (3) Ultrasonic waves are generated in LIPS experiments through direct coupling between the em and acoustic fields. Heating through optical absorption is not responsible for acoustic wave generation, as determined by experiment. (4) The LIPS technique has a wide range of applications in many fields. Some applications in chemical physics, optics, and acoustics are discussed.

II. THE NATURE OF THE ACOUSTIC EFFECT

Here we discuss experimental results which verify Eq. (1) as the correct description of the acoustic response to the crossed laser excitation pulses. The conclusions are drawn strictly from experimental data and do not rely on a specific model for the mechanism of phonon generation. This discussion is to establish that a correct theoretical description of the LIPS excitation process must predict the acoustic effect given in Eq. (1).

The top of Fig. 2 shows LIPS data taken on pentacene in p-terphenyl with 532.0-nm excitation and 596.0-nm probe pulses. The diffracted signal contains an exponentially decaying component, due to the excited-state concentration grating, which is periodically increased due to the phonon-induced spectral shifts. The period of the modulated signal τ = 0.95 ns and the acoustic wavelength, determined as in Fig. 1, is $\Lambda = 2.44$ μm. The speed of sound $v_p = \Lambda/\tau_{ac} = 2.57 \times 10^5$ cm/sec, in good agreement with the conventionally measured value.[8] The important feature to notice is that the periodically modulated part of the signal vanishes exactly once each acoustic cycle. If the acoustic disturbance consisted of only a standing wave (no density offset), the modulation would vanish twice each acoustic cycle.

The second sweep in Fig. 2 shows LIPS data on the same crystal under identical experimental conditions as the first except with a 581.0-nm probe wavelength. The diffracted signal contains an exponentially decaying component, due to the excited-state concentration grating, which is periodically *decreased* due to the phonon-induced spectral shifts. The pentacene in p-terphenyl spectrum (inset, Fig. 2) shows that 596.0 nm lies to the red of the absorption maximum and 581.0 nm lies to the blue. The probe wavelength dependence exhibited in Fig. 2 is discussed immediately below and demonstrates that the material density in the grating peaks oscillates between normal and a reduced value, while the density in the grating nulls oscillates between normal and an in-
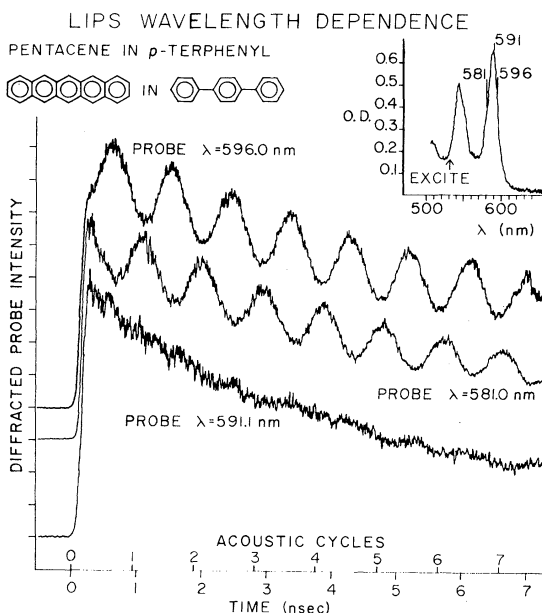
FIG. 2. LIPS probe wavelength dependence in p-terphenyl. The oscillating component of the signal increases when the probe wavelength is red of the pentacene absorption peak (see inset), decreases when the probe wavelength is blue of the absorption peak, and vanishes when the probe wavelength is at the peak. This demonstrates that the oscillations are caused by phonon-induced shifts in the pentacene absorption spectrum, and that the acoustic disturbance is correctly described by Eq. (1); see text. All experiments were done with identical excitation conditions.

creased value. This is the behavior described by Eq. (1). A pure standing wave would result in density oscillations above and below normal in both the peaks and the nulls.

In these experiments absorption of the 532-nm excitation pulses at the interference maxima (the grating peaks) set up an excited-state concentration grating. The total diffraction due to superimposed population and spectral shift gratings is calculated quantitatively in the next section. For the purposes of this qualitative discussion, we need to note that the grating's diffracting power is proportional to the square of the difference in optical density (OD) at the grating peaks and the grating nulls. The probe wavelength is absorbed only by the ground states, so the excited-state concentration grating has a higher OD in the grating nulls than in the grating peaks. In pentacene in p-terphenyl, as in most organic molecular crystals, the $S_0 \rightarrow S_1$ absorption spectrum red shifts with increasing density.[3] Equation (1) then predicts that the spectrum will periodically red shift in the grating nulls and blue shift in the grating peaks. If the probe wavelength lies to the red of the $S_0 \rightarrow S_1$ absorption maximum, the

periodic spectral shifts will *increase* the OD in the grating nulls and *decrease* the OD in the grating peaks. This increases the peak-null OD difference above that due to the excited-state concentration grating alone. Diffracted signal will therefore be periodically *increased* above that due to the excited-state concentration grating. Thus, when the probe wavelength lies to the red of the absorption maximum, the diffracted signal is periodically increased, as in the top trace in Fig. 2. If the probe wavelength lies to the blue of the absorption maximum, the periodic spectral shifts *decrease* the OD in the grating nulls and *increase* the OD in the grating peaks, opposing the effect of the excited-state concentration grating and periodically *reducing* diffracted signal. Thus when the probe wavelength lies to the blue of the absorption maximum, the diffracted signal is periodically reduced, as in the second trace in Fig. 2. A pure standing wave could not cause this probe wavelength dependence since material in both the peaks and the nulls would oscillate between increased and decreased density, leading to blue and red spectral shifts in both peaks and nulls. Diffracted signal would then oscillate above *and* below that due to the excited-state concentration grating alone, regardless of probe wavelength. This is not observed in a wide variety of samples under a range of experimental conditions. Thus the time dependence and probe wavelength dependence of the diffracted signal clearly verify Eq. (1) as the correct description of the acoustic disturbance, i.e., a static density offset and a standing wave must be present.

III. THEORETICAL

A. Diffraction from superimposed population and spectral shift gratings

In this section we calculate transient grating diffracted signal (s) due to the combined effects of a sinusoidal excited-state population distribution and a time-dependent sinusoidal density variation which produces spectral shifts. Both effects have been treated in detail separately.[5,9] The results will show how spectral shifts can be directly measured from LIPS transient grating data.

Bragg diffraction of a probe pulse of frequency ν from a sinusoidally varying optical-density pattern is proportional to the square of the difference in optical density (OD) at the grating peaks and the grating nulls[9,10]:

$$s(\nu) \propto [\mathrm{OD}(\nu, \mathrm{peak}) - \mathrm{OD}(\nu, \mathrm{null})]^2. \qquad (4)$$

Optical density at frequency ν is given by

$$\mathrm{OD}(\nu) = \epsilon(\nu) b c, \qquad (5)$$

where $\epsilon(\nu)$ is the molar extinction coefficient at frequency ν, b is the sample thickness, and c is the concentration of absorbing species (ground-state pentacene molecules in these experiments). The transient grating diffracted signal arises from spatial variation in both $\epsilon(\nu)$ and c.

The LIPS excitation conditions result in a spatially varying, sinusoidal distribution of excited states imaging the optical-interference pattern

$$N_1(y,t) = \frac{N_{1\max}}{2}(1+\cos ky)e^{-t/\tau}, \tag{6}$$

where $N_{1\max} = N_1(0,0)$ is the excited-state concentration at the grating peaks at $t=0$ (assuming instantaneous excitation), τ is the excited-state lifetime, and k is the grating wave vector determined by the wavelength and orientation of the excitation pulses (see Fig. 1). In these experiments the probe wavelength lies within the $S_0 \to S_1$ absorption profile and is not absorbed by the excited states, so the sinusoidally varying ground state concentration $N_0(y,t)$ results in a TG signal which, according to Eqs. (4) and (6), decays with one-half the excited-state lifetime.

The excitation pulses also generate an acoustic disturbance described by Eq. (1). We will assume that the grating wave vector is aligned along a pure mode direction of the crystal, so that only longitudinal waves are generated. The necessary considerations to obtain the general case have been presented in detail previously.[5] The local density change $\delta\rho$ at any point in the crystal is related to the instantaneous strain at that point by Eq. (3). We now assume that the small density changes occurring in LIPS experiments shift the $S_0 \to S_1$ absorption profile linearly with density. For a Gaussian absorption profile,

$$\epsilon(\nu) = \epsilon_{\max} e^{-B^2(\nu-\nu_B)^2}, \tag{7}$$

where $1/B$ is the half-width and ν_B is the density-dependent absorption maximum,

$$\nu_B = \nu_B^0 + \gamma(\delta\rho). \tag{8}$$

ν_B^0 is the absorption maximum at normal density and γ is the spectral shift per unit density change in the linear approximation. From Eqs. (1), (3), and (8),

$$\nu_B = \nu_B^0 + \nu_S \cos ky(1-\cos\omega t) = \nu_B^0 + \nu_B' \cos ky, \tag{9}$$

where $2\nu_S = -2\gamma\rho_0 A$ is the maximum spectral shift and $\nu_B'(t) = \nu_S(1-\cos\omega t)$. (Note that for an absorption profile which red shifts with increasing density, $\gamma < 0$ and $\nu_S > 0$.) Substituting Eq. (9) into Eq. (7) gives the density-dependent extinction coefficient,

$$\epsilon(\nu,\rho) = \epsilon(\nu,y,t) = \epsilon_{\max} e^{-B^2(\nu-\nu_B^0-\nu_B'\cos ky)^2}. \tag{10}$$

For broad spectral lines, such as those involved in room-temperature pentacene in p-terphenyl LIPS experiments, the spectral shifts are about $1\ \text{cm}^{-1}$ while the absorption linewidth $1/B$ is $170\ \text{cm}^{-1}$. It is then valid to approximate Eq. (10) as

$$\epsilon(\nu,y,t) = \epsilon_{\max} e^{-B^2(\nu-\nu_B^0)^2}[1 + 2B^2(\nu-\nu_B^0)\nu_B'\cos ky]. \tag{11}$$

This gives a sinusoidal variation in extinction coefficient. According to Eq. (4), this variation (in the absence of a spatial variation in the ground-state concentration) results in transient grating signal which is periodically modulated due to the $\nu_B' = \nu_S(1-\cos\omega t)$ term.

We now calculate TG signal due to both density and population effects. Equations (5), (6), and (11) give

$$OD(\nu,y,t) = \epsilon_{\max} e^{-B^2(\nu-\nu_B^0)^2} Nb \left\{ 1 - \frac{N_{1\max}}{2N} e^{-t/\tau}[1 + B^2(\nu-\nu_B^0)\nu_B'] \right.$$

$$+ \left[2B^2(\nu-\nu_B^0)\nu_B'\left(1 - \frac{N_{1\max}}{2N}e^{-t/\tau}\right) - \frac{N_{1\max}}{2N}e^{-t/\tau} \right]\cos ky$$

$$\left. - \frac{N_{1\max}}{2N}B^2(\nu-\nu_B^0)\nu_B'e^{-t/\tau}\cos 2ky \right\}, \tag{12}$$

where $N = N_0 + N_1$ is the total concentration of the molecule of interest. The $\cos 2ky$ term has a negligible contribution to the first-order diffracted spot when the probe pulse enters at the Bragg angle appropriate for diffraction by a grating with wave vector k.[11] Ignoring this term leaves a sinusoidally varying OD from which the TG signal can be calculated from Eq. (3). This gives

$$s(\nu,t) \propto a\left[2B^2(\nu-\nu_B^0)\nu_S(1-\cos\omega t)\left(1 - \frac{N_{1\max}}{2N}e^{-t/\tau}\right) \right.$$

$$\left. - \frac{N_{1\max}}{2N}e^{-t/\tau} \right]^2, \tag{13}$$

where $a = (2\epsilon_{\max}e^{-B^2(\nu-\nu_B^0)^2}Nb)^2$.

The first term in Eq. (13) describes density-

dependent spectral shift effects on the TG signal. This term vanishes at $\omega t = 0, 2\pi, 4\pi, \ldots$ (at $t = 0$, $\tau_{ac}, 2\tau_{ac}, \ldots$, where τ_{ac} is the duration of one acoustic cycle). At these times the density is uniform throughout the sample [see Eq. (1)], there are no spectral shifts, and the TG signal is due entirely to the concentration distribution whose effects are described by the second term in Eq. (13). The spectral shifts and their effects on the TG signal are largest at $t = \frac{1}{2}\tau_{ac}, \frac{3}{2}\tau_{ac}, \ldots$, i.e., when the density excursion in the sample is the greatest.

Equation (13) quantitatively verifies the qualitative considerations of Sec. II. For $\nu_S > 0$ (i.e., a spectrum which red shifts with increasing density) and $\nu - \nu_B^0 < 0$ (probe wavelength red of the absorption maximum), the spectral shifts periodically *increase* the TG signal above that due to the concentration grating alone. For $\nu_S > 0$ and $\nu - \nu_B^0 > 0$ (probe wavelength blue of the absorption maximum) the spectral shifts *decrease* the TG signal below that due to the concentration grating alone. As discussed in Sec. II, this is expected since at normal density the ground-state population and OD's are higher in the grating nulls than in the grating peaks. As density increases (spectrum red shifts) in the nulls, and density decreases (spectrum blue shifts) in the peaks, the peak-null difference in OD (and therefore TG signal) *increases* for a probe-frequency red of the absorption maximum and *decreases* for a probe-frequency blue of the absorption maximum.

It should be mentioned that LIPS data with the probe-wavelength blue of the absorption maximum, in which the spectral shifts cause a *reduction* of total diffracted signal (Fig. 2), guarantee that diffraction is due to variation in optical density, i.e., an amplitude grating, rather than due to a phase grating (variation in the real part of the index of refraction). This is so since a phase grating superimposed upon an amplitude grating can only *increase* the grating's total diffracting power.[10,12]

The magnitude of the density-dependent spectral shift ν_S is easily extracted from the time-dependent transient grating data by measuring the amplitude of the modulations. The simplest procedure is to compare the TG signal at $t = n\tau_{ac}$ (no spectral shift) and at $t = (n + \frac{1}{2})\tau_{ac}$ (maximum spectral shift). From Eq. (13),

$$\left(\frac{s[(n + 1/2)\tau_{ac}]}{s(n\tau_{ac})}\right)^{1/2} = e^{-\tau_{ac}/2\tau}\left[1 - 4B^2(\nu - \nu_B^0)\nu_S\left(\frac{2Ne^{(n+1/2)\tau_{ac}/\tau}}{N_{1max}} - 1\right)\right], \tag{14}$$

and solving for the spectral shift ν_S,

$$\nu_S = \frac{1 - \left(\dfrac{s[(n + \frac{1}{2})\tau_{ac}]}{s'(n\tau_{ac})}\right)^{1/2}}{4B^2(\nu - \nu_B^0)\left(\dfrac{2Ne^{(n+1/2)\tau_{ac}/\tau}}{N_{1max}} - 1\right)}, \tag{15}$$

where $s'(n\tau_{ac}) = s(n\tau_{ac})e^{-\tau_{ac}/\tau}$ is the value that $s[(n + \frac{1}{2})\tau_{ac}]$ would assume in the absence of spectral shift effects. In practice, $s'(n\tau_{ac})$ can be accurately determined directly from the data.

Equation (15) allows the direct computation of ν_S, the density-dependent spectral shift, from LIPS transient grating data. Typically, N_{1max}/N is determined for each TG data set by measuring the change in transmitted probe pulse intensity when the probe pulse is immediately preceded by one of the excitation pulses. Variably delaying the probe pulse permits measurement of the lifetime τ. The acoustic cycle τ_{ac} is directly measured from the time-dependent TG data, and B and ν_B^0 are measured spectroscopically. Thus ν_S, the spectral shift, can be determined.

B. Electrostriction and optical generation of acoustic waves

In this section we consider direct electrostrictive coupling of the em field of the crossed laser pulses and the acoustic field of the sample. As explained in Sec. II the acoustic disturbance produced in LIPS experiments consists of counterpropagating waves plus a static density offset, described by Eq. (1). We show here that the theory of electrostriction predicts generation of an acoustic disturbance consisting of counterpropagating waves and a static density offset. However, the density offset occurs during the time that the excitation pulses are in the crystal and is predicted to disappear after the pulses leave the crystal. This is in direct contrast to experimental results which clearly demonstrate the continued presence of the density offset. Thus the theory of electrostriction does not predict the complete acoustic response. As will be shown, the theory does not account for the accumula-

tion of heat in the sample as the pulses pass through it, and in this sense appears deficient.

Electrostrictive generation of high-amplitude, narrow-band traveling waves in condensed media has been demonstrated by several workers.[13] The basic scheme has been to cross two laser beams of slightly different frequency in the medium, with phonons of the difference frequency and wave vector being generated. Quantum mechanically, stimulated Brillouin scattering[13,14] annihilates photons from the higher-frequency beam and creates photons in the lower-frequency beam and acoustic phonons in the medium. Since the phonon frequency ω_p and wave vector k_p must satisfy the dispersion relation of the medium $(\omega_p/k_p = v_p$, the speed of sound), only one angle of intersection between the two beams is acceptable for the process to occur effectively. The efficiency of phonon generation has been found to be extremely sensitive to small deviations from the correct angle.[13] The technique does not allow one to tune over a range of phonon frequencies.

In the transient grating laser-induced phonon method, short pulses centered at the same frequency are employed. The spread in frequency is broad enough to allow efficient phonon generation at any angle of intersection. Higher-frequency photons from one beam are Brillouin scattered to give lower-frequency photons (still within the laser linewidth) in the other beam and phonons of the difference frequency and wave vector in the medium.

The coupling between the incident em field and the sample's acoustic field is conveniently described by the interaction Lagrangian,[15]

$$L_{\text{int}} = -\frac{1}{8\pi} \sum_{ijkl} p_{ijkl} D_i D_j \frac{\partial u_k}{\partial x_l} , \tag{16}$$

where the D_i are components of the electric displacement vector, p_{ijkl} are photoelastic (elasto-optic) constants, and u_k are displacements. The photoelastic constants relate the optical and mechanical responses of the medium by

$$\delta\nu_{ij} = \sum_{kl} p_{ijkl} \frac{\partial u_k}{\partial x_l} , \tag{17}$$

where ν_{ij} are components of the reciprocal dielectric tensor.

The Lagrangian (16) leads to the following equations of motion describing the acoustic and em fields[15]:

$$\rho \ddot{u}_i + \sum_j \eta_{ij} \dot{u}_j - \sum_{jkl} \lambda_{ijkl} \frac{\partial^2 u_l}{\partial x_j \partial x_k}$$

$$= \sum_{jkl} \frac{1}{8\pi} p_{klji} \frac{\partial}{\partial x_j} D_k D_l , \tag{18}$$

$$\frac{1}{c^2} \ddot{D}_i - \sum_{jk} \nu_{kj} \left(\delta_{ik}\nabla^2 - \frac{\partial}{\partial x_i}\frac{\partial}{\partial x_k} \right) D_j$$

$$= \sum_{kjlm} p_{kjlm} \left(\delta_{ik}\nabla^2 - \frac{\partial}{\partial x_i}\frac{\partial}{\partial x_k} \right) D_j \frac{\partial u_l}{\partial x_m} , \tag{19}$$

where ρ is the material density, η_{ij} are acoustic damping constants, and λ_{ijkl} are elastic stiffness coefficients. The equations of motion (18) and (19) do not consider changes in temperature caused by the applied em field. Heating effects will be dealt with below.

We assume that the intense excitation pulses are not significantly affected by the acoustic field, so Eq. (19), which describes the effect of the acoustic field on the em field, does not concern us. Equation (18) describes the response of the acoustic field to the em driving force.

To solve the acoustic wave Eq. (18), we use the coordinate system shown in Fig. 1. The exposed crystal face defines the x_1x_2 plane, and the two incoming beams are in the x_2x_3 plane with the x_3 axis bisecting them. We further assume the pulses to be x_1 polarized, fixing $D_2 = D_3 = 0$ in Eq. (18). Choosing other polarizations does not qualitatively affect the results.

A laser pulse traveling in the x_3 direction in the crystal is described by integrating over the Gaussian spread of frequencies,

$$\hat{x}_1 D e^{-(x_1^2+x_2^2)/\omega_0^2} \int_{-\infty}^{\infty} e^{-[(\omega-\omega_L)/\Gamma]^2} \cos[\omega(t-t_0) - kx_3]\,d\omega$$

$$= \hat{x}_1 D\pi^{1/2}\Gamma e^{-(x_1^2+x_2^2)/\omega_0^2} e^{-(t-t_0-x_3 n/c)^2\Gamma^2/4}$$

$$\times \cos[\omega_L(t - t_0) - k_3 x_3] , \tag{20}$$

where D is the maximum amplitude, ω_0 is the spot size, t_0 determines when the pulse passes through the crystal, c/n is the speed of light in the medium, ω_L is the central frequency, $k_3 = k(\omega_L)$, and Γ is the spectral width. (The transform limited pulse duration is $2/\Gamma$.) The two pulses crossing inside the crystal are described by

$$\hat{x}_1 E e^{-(t-t_0)^2\Gamma^2/4}\cos[\omega_L(t - t_0) \pm k_2 x_2 - k_3 x_3] , \tag{21}$$

where $E = D\pi^{1/2}\Gamma$. We are primarily concerned with the center of the interaction region, so we ignore the transverse spatial variation of the pulses. The position of the sample has been set at $x_3 = 0$ and sample thickness (typically about 100 μm) has been ignored.

From Eq. (21) the total em field intensity due to both pulses is

$$D_1^2 = E^2 e^{-(t-t_0)^2\Gamma^2/2}\{1 + \cos 2[\omega_L(t - t_0) - k_3 x_3]$$

$$\times (1 + \cos 2k_2 x_2) + \cos 2k_2 x_2\} , \tag{22}$$

and this is inserted into the driving term on the right-hand side of Eq. (18). The first term in the brackets in (22) can be discarded since its spatial derivatives vanish. Retaining the second term, which oscillates at optical frequencies, shows that it does not effectively drive the acoustic field. Only the third term produces a significant acoustic response. Keeping only this term reduces the right-hand side of Eq. (18) to

$$\frac{1}{8\pi}\sum_j p_{11ji}\frac{\partial}{\partial x_j}\ E^2 e^{-(t-t_0)^2\Gamma^2/2}\ \cos 2k_2 x_2$$

$$= -\frac{k_2}{4\pi}\ p_{112i}'E^2 e^{-(t-t_0)^2\Gamma^2/2}\ \sin 2k_2 x_2\ .\quad (23)$$

To simplify the solution of Eq. (18) we assume the grating to be aligned along a symmetry-determined pure mode direction of the crystal, i.e., we assume that pure longitudinal and transverse waves can propagate in the x_2 direction. Then the photoelastic constant p_{112i} vanishes for $i\neq 2$. (Note that the photoelastic tensor has the same nonzero elements as the elastic stiffness tensor.[6]) Then Eq. (18) becomes

$$\rho \ddot{u}_2 - \sum_{jkl}\lambda_{2jkl}\frac{\partial^2 u_l}{\partial x_j \partial x_k}$$

$$= -\frac{k_2}{4\pi}p_{1122}E^2 e^{-(t-t_0)^2\Gamma^2/2}\ \sin 2k_2 x_2 \quad (24)$$

and

$$\rho \ddot{u}_i - \sum_{jkl}\lambda_{ijkl}\frac{\partial^2 u_l}{\partial x_j \partial x_k}\ = 0 \quad (25)$$

for $i=1,3$. Acoustic loss has been neglected since it should be negligible on the time scale of interest (~10 ns). These equations can be satisfied by one wave, a longitudinal wave in the x_2 direction. This leaves

$$\ddot{u}_2 - v_p^2 \frac{\partial^2 u_2}{\partial x_2^2} = -\frac{k_2 p_{1122}}{4\pi\rho}\ E^2 e^{-(t-t_0)^2\Gamma^2/2}\ \sin 2k_2 x_2\ , \quad (26)$$

where $v_p =(\lambda_{2222}/\rho)^{1/2}$ is the longitudinal wave velocity. Note that if the x_2 direction is not a pure mode direction of the crystal, Eq. (18) is more complicated and has a solution involving multiple waves. This type of problem was dealt with in

detail in the original LIPS treatment[5] which assumed a coupling mechanism involving optical absorption and heating. In that treatment, the sinusoidal temperature distribution results in a driving term identical in form to that in Eq. (23), except time independent. Both treatments predict generation of the same types of counterpropagating waves for any grating alignment. For arbitrary grating alignments in a crystal three waves, one quasilongitudinal and two quasitransverse, will be generated. Along pure mode directions, pure transverse waves will be excluded. Results of LIPS experiments in which two waves, one quasilongitudinal and one quasitransverse, were generated are shown below. The solution of Eq. (26) is given by

$$u_2(x_2,t)=\frac{1}{2v_p}\int_0^t \int_{x_2-v_p(t-t')}^{x_2+v_p(t-t')} f(x',t_2')dx_2' dt'\ , \quad (27)$$

where $f(x_2',t')$ is the driving term on the right-hand side of Eq. (26). To do the integral and examine the acoustic field at any time, we treat the em field as a square pulse in time instead of a Gaussian. The result suggests that this causes no qualitative changes. Replacing the exponential in Eq. (26) by a square pulse which begins at $t=0$ gives

$$u_2(x_2,t)=-\frac{p_{1122}E^2}{16\pi k_2\rho v_p^2}\ \sin 2k_2 x_2 (1-\cos 2k_2 v_p t) \quad (28)$$

and

$$S_{22}=\frac{\partial u_2}{\partial x_2}=-\frac{p_{1122}E^2}{8\pi\rho v_p^2}\cos 2k_2 x_2 (1-\cos 2k_2 v_p t)$$

$$=-\frac{p_{1122}E^2}{8\pi\rho v_p^2}\{\cos 2k_2 x_2 -\tfrac{1}{2}[\cos 2k_2(v_p t -x_2)$$

$$+\cos 2k_2(v_p t +x_2)]\} \quad (29)$$

for $t<\tau_L$, the laser square-pulse duration. Thus, during the laser pulse the acoustic field consists of counterpropagating waves and a static density offset, exactly as in Eq. (1). Notice, however, that the amplitude of the acoustic disturbance *remains constant* throughout the duration of the pulse. Calculation of the acoustic field after the end of the square-pulse driving force $(t>\tau_L)$ gives

$$S_{22}(x_2,t>\tau_L)=\frac{p_{1122}E^2}{16\pi\rho v_p^2}([\cos 2k_2(v_p t -x_2)+\cos 2k_2(v_p t +x_2)]$$

$$-\{\cos 2k_2[v_p(t-\tau_L)-x_2]+\cos 2k_2[v_p(t-\tau_L)+x_2]\})\ , \quad (30)$$

showing that the static density term disappears when the pulses leave the crystal. The additional set of counterpropagating waves in Eq. (30) is actually an artifact of the square-pulse treatment;

if the Gaussian pulse shape is retained in Eq. (26), the acoustic field can be calculated from Eq. (27) at any time *after* the pulses leave the crystal, since then the limits on the integral over time can

be taken as $\pm\infty$. This yields

$$S_{22}(x_2, t \gg 2/\Gamma) = -\frac{k_2 p_{1122} E^2}{2^{5/2}\pi^{1/2} v_p \rho \Gamma} e^{-2k_2^2 v_p^2/\Gamma^2}$$

$$\times\{\sin 2k_2[v_p(t - t_0) + x_2]$$

$$+ \sin 2k_2[v_p(t - t_0) - x_2]\}, \quad (31)$$

i.e., a single set of counterpropagating waves.

Examination of the square-pulse solution is useful, however, because it illustrates a crucial feature of the theoretical prediction: The amplitude of the acoustic disturbance does not continually increase throughout the duration of the pulses. The theory may be modified to consider heating effects and variations in temperature.[7,16] In this case the acoustic field Eq. (18) is most easily solved in terms of strain rather than displacement. As before, acoustic loss and optical frequency em driving terms are neglected and the x_2 direction is taken to be a pure mode direction. The acoustic field equation then becomes

$$\frac{\partial^2 S_{22}}{\partial t^2} - \frac{v_p^2}{\gamma}\frac{\partial^2 S_{22}}{\partial x_2^2} + \frac{v_p^2 \alpha_{22}}{\gamma}\frac{\partial^2 T}{\partial x_2^2}$$

$$= \frac{p_{1122}}{8\pi\rho_0}\frac{\partial^2 D_1^2}{\partial x_2^2} + \frac{\partial}{\partial x_2}\left[\frac{D_1^2}{8\pi\rho_0}\left(\frac{\partial \nu_{11}}{\partial T}\right)_S \frac{\partial T}{\partial x_2}\right], \quad (32)$$

where γ is the ratio of specific heats, α_{22} is the coefficient of linear thermal expansion in the x_2 direction, and $\underline{S}$ is the strain tensor. The term on the far right is due to the electrocaloric effect. This effect is often negligible since usually

$$p_{1122} = \left(\frac{\partial \nu_{11}}{\partial S_{22}}\right)_T \gg \left(\frac{\partial \nu_{11}}{\partial T}\right)_{\underline{S}}.$$

The heat conduction equation is

$$\rho_0 c_V \frac{\partial T}{\partial t} - \mathcal{K}_{22}\frac{\partial^2 T}{\partial x_2^2} + \frac{\rho_0 c_V(\gamma - 1)}{\alpha_{22}}\frac{\partial S_{22}}{\partial t} = \frac{dQ}{dt}, \quad (33)$$

where c_V is the constant volume heat capacity, $\mathcal{K}_{22}$ is the thermal conductivity in the x_2 direction, and Q is the heat per unit volume applied to the medium. Owing to the electrocaloric effect,

$$\frac{dQ}{dt} = -\frac{1}{8\pi}T_0\left(\frac{\partial \nu_{11}}{\partial T}\right)_{\underline{S}}\frac{\partial D_1^2}{\partial t}, \quad (34)$$

where T_0 is the unperturbed temperature of the medium. Neglecting thermal conductivity, which is negligible on this time scale, Eq. (33) becomes

$$\frac{\partial T}{\partial t} + \frac{\gamma - 1}{\alpha_{22}}\frac{\partial S_{22}}{\partial t} = -\frac{1}{8\pi\rho_0}\frac{T_0}{c_V}\left(\frac{\partial \nu_{11}}{\partial T}\right)_{\underline{S}}\frac{\partial D_1^2}{\partial t}. \quad (35)$$

Equations (32) and (35) must be solved to calculate the acoustic response to the em field. Our real concern is the form of this response shortly after the pulses pass through the crystal, at which time the driving terms on the right-hand sides of both equations vanish. It is then immediately

apparent that the solutions will be of the same form as those found earlier [Eq. (31)]. Inspecting Eq. (34), we see that no net heat is deposited into the medium by the em field through the electrocaloric effect. When $\partial(D_1^2)/\partial t$ is positive, i.e., as the pulses enter the crystal, heat is put into the medium, and when $\partial(D_1^2)/\partial t$ is negative, i.e., as the pulses leave the crystal, the same amount of heat is taken from the medium. Thus there is no long-lived temperature increase. The electrocaloric effect can be viewed as resulting from a change in pressure at constant volume. The pressure and temperature rise while the pulses are passing through the crystal, then return to their original values as the pulses leave.

From Eq. (35) the only other variation in temperature is due to the adiabatic propagation of the acoustic waves (the second term on the left). After the pulses leave the crystal, Eqs. (32) and (35) show that both strain and temperature are of the form of Eq. (31), i.e., a single set of counterpropagating waves. The only difference between this and the earlier result is that the temperature variations due to adiabatic acoustic wave propagation are explicitly accounted for.

The problem with the theory is that it accounts for no net heat deposited into the crystal by the em field. Yet the experimental results clearly demonstrate that there is a static density offset which must arise from some form of heating mechanism. If optical absorption were included, Eq. (34) would have an additional term proportional to the absorption coefficient and to D_1^2.[16] This would clearly produce the desired result, namely a nonpropagating, long-lived temperature variation which builds up throughout the pulse duration. The original theoretical treatment of this experiment considered only the optical-absorption driving term. However, the experiments described below show conclusively that absorptive heating is not an important phenomenon. We propose that a term in D_1^2 should still be included in Eq. (34), but related to stimulated scattering rather than absorption. This would represent heating by direct coupling of the em field to incoherent phonons of various frequencies. That such coupling occurs can be shown by returning to Eq. (20), which describes the laser pulses in terms of their distribution of frequencies. If instead of integrating over all frequencies as in Eq. (20), one considers a single frequency from one pulse and another single frequency from the other pulse, treating the electrostriction problem with only these frequencies in the driving term shows an acoustic response at the difference frequency. The sum of these responses, over all the frequencies in both excitation pulses, produces an

ensemble of incoherent phonons which should be
responsible for the observed density offset. How-
ever, existing theory fails to predict the growth of
the offset (heating) throughout the duration of the
excitation or the continued presence of the offset
after excitation. The LIPS experiment allows ob-
servation of the detailed nature of the acoustic
disturbance. This permits a critical evaluation
of theoretical treatments of em and acoustic field
interactions.

IV. EXPERIMENTAL

The LIPS experimental setup is illustrated in
Fig. 3. The laser is a continuously pumped
Nd:YAG (YAG denotes yttrium aluminum garnet)
system which is acousto-optically mode locked
and Q switched to produce high-repetition-rate
(200 Hz), high-power infrared (1.06 μm) pico-
second pulses. The laser output is a train of about
40 mode-locked pulses, 5.7 ns apart, with ~1.4
mJ total energy. A large pulse from the train
is selected by a Pockels cell with avalanche trans-
istor driver. The single pulse is frequency doub-
led by means of a deuterated cesium dihydrogen
arsenate crystal (CD*A) to give a 20-μJ, 80-ps,
transform-limited TEM_{00} pulse at 532 nm. This
passes through a 50%-beam splitter to create
the two excitation pulses, which travel equal dis-
tances and are focused into the sample. In some
experiments tripled YAG 355-nm excitation pulses
were used. A rubidium dihydrogen phosphate
(RDP) sum generating crystal produced 6-μJ
pulses at 355 nm.

The unused IR pulse train comes off a reflecting
polarizer into another CD*A doubler crystal,
and the 532-nm light is used to synchronously
pump a dye laser which is spectrally narrowed
and tuned by two intracavity etalons. The dye
laser is cavity dumped using another Pockels
cell with avalanche transistor driver to give an
8-μJ, 30-ps pulse with a spectral width of ~1 cm^{-1}.
Synchronization of the two Pockels cells is ob-
tained by a single avalanche transistor which it-
self is triggered by the IR pulse train. The dye
laser output travels a variable distance controlled
by a motorized delay line consisting of a corner
cube drawn along a precision optical rail. It
probes the grating at an angle satisfying the Bragg
diffraction condition. Typical excitation and probe
spot sizes were 250 and 150 μm, respectively.

The diffracted probe intensity was measured
with a p-i-n photodiode and lock-in amplifier
which drives the y axis of an x-y recorder. The
x axis is driven by a variable voltage derived
from a 10-turn potentiometer connected to the
delay line motor, providing the time scale. When
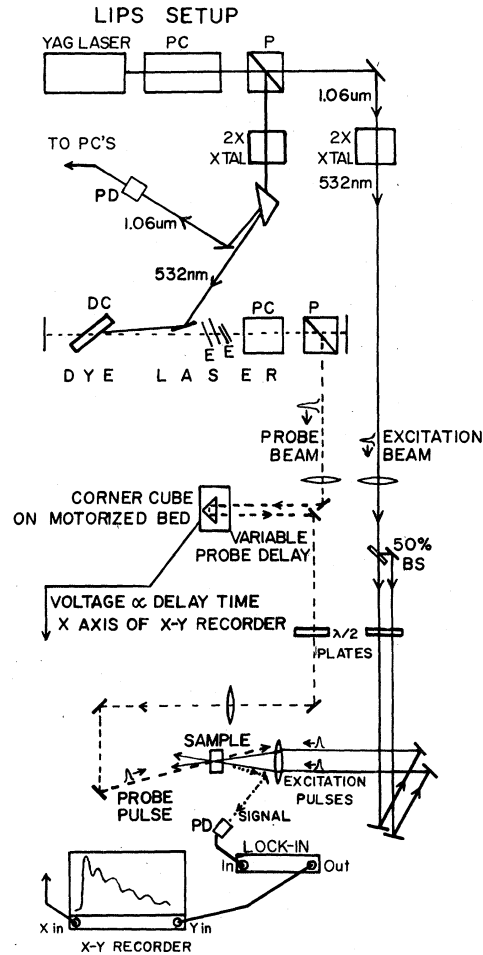the delay line is run, the time-dependent diffract-

FIG. 3. Transient grating experimental setup. A
single 1.06-μm pulse is selected from the YAG mode-
locked pulse train and frequency doubled to 532 nm,
then split into the two excitation pulses and recombined
at the sample to generate the counterpropagating waves
and transient grating. The rest of the pulse train is
frequency doubled to synchronously pump a tunable dye
laser whose output probes the grating after a variable
delay. The Bragg-diffracted part of the probe pulse
is the transient grating signal. $PC \equiv$ Pockels cell;
$P \equiv$ polarizer; $PD \equiv$ photodiode; $DC \equiv$ dye cell; $E \equiv$
etalon; $BS \equiv$ beam splitter.

ed signal is recorded directly on the x-y recorder.

In all experiments the excitation pulse intensity
was measured to determine the number of ex-
cited states produced. Knowledge of $N_{1\,max}/N$ is
necessary to calculate spectral shifts from LIPS
data as in Eq. (15). Taking saturation effects
into account,

$$\frac{N_{1\,max}}{N} = 1 - e^{\sigma E_{max}}, \qquad (36)$$

where E_{max} is the number of photons crossing
a unit area at the grating peaks and σ is the ab-

sorption cross section measured spectroscopically. For pentacene in p-terphenyl, a-axis-polarized light striking the ab face of a crystal has $\sigma(532$ nm$) = 2.0 \times 10^{-17}$ cm^2 and $\sigma(355$ nm$) = 1.3 \times 10^{-17}$ cm^2.

The ratio of incident and transmitted probe pulse intensities was also measured for each experiment by pickoffs into p-i-n photodiodes. Measurement of this ratio with the dye laser tuned off the pentacene absorption profile provided a correction for reflection and scattering losses; the absolute OD at any dye laser wavelength could then be determined, and dye laser spectra were taken at each spot in a sample on which LIPS experiments were performed. By measuring the sample thickness, the local pentacene concentration at each spot could be calculated. The transmitted probe intensity was also measured when the probe pulse was immediately preceded in the sample by one excitation pulse. This provided an experimental check on the calculation of $N_{1\text{max}}/N$ described above, since

$$\frac{N_1}{N} = 1 - \frac{\text{OD}^*}{\text{OD}}, \tag{37}$$

where $\text{OD}^* = -\log_{10} I^*/I_0$ and I^* is the intensity of the transmitted probe pulse preceded in the sample by one excitation pulse. $N_{1\text{max}}/N$ is calculated from Eq. (37), correcting for the fact that the excitation intensity at the grating peaks is four times the intensity of a single pulse. Typically, calculated and measured values of $N_{1\text{max}}/N$ agreed within 5%.

Pentacene in p-terphenyl samples were obtained by recrystallizing and extensively zone refining (> 200 passes) p-terphenyl (Eastman Scintillation Grade), adding various concentrations of pentacene (Aldrich), and growing crystals under vacuum by the Bridgman technique. Single crystals were cleaved along the ab plane to yield samples ranging in thickness from 50 μm to 3 mm. Fluorene single crystals were obtained from commercial material (Eastman) using the same procedure. Perylene single crystals were obtained by extensively (> 200 passes) zone refining commercial material (Aldrich 99%), selecting the central zones, and again zone refining. The purest zones were used to grow α-perylene single crystals under vacuum by the Bridgman technique and β-perylene crystals by slow evaporation of benzene from a saturated solution.

V. RESULTS AND DISCUSSION

LIPS experiments on pentacene in p-terphenyl crystals were performed with constant excitation conditions (therefore constant spectral shift magnitude ν_S) and a variety of probe wavelengths

to verify the wavelength-dependence predicted by Eq. (15). Qualitative verification has already been provided in Fig. 2, which shows that for $\nu < \nu_B^0$ (red probe) the TG signal is periodically increased, $\nu > \nu_B^0$ (blue probe) the TG signal is periodically decreased, and for $\nu = \nu_B^0$ (probe at absorption peak) the TG signal has no periodic component. (Note that $\nu_S > 0$ for pentacene in p-terphenyl, whose absorption spectrum red shifts with increasing density.) Equation (15) predicts that as the probe wavelength is tuned away from the absorption maximum, i.e., as $|\nu - \nu_B^0|$ increases, the amplitudes of the modulations increase. Figure 4 shows results of a series of experiments on a 2.9×10^{-5} M/M crystal with identical excitation conditions and probe wavelengths spanning the red side of the absorption spectrum. The predicted linear dependence of $1 - [s(\frac{1}{2}\tau_{ac})/s'(0)]^{1/2}$ on $(\nu_B^0 - \nu)$ is observed. Application of Eq. (15) yields a value of $\nu_S = 6.9$ cm$^{-1} \pm 5\%$ for all wavelengths. Similar results have been obtained on numerous samples with a wide range of concentrations.

The dependence of ν_S on excitation intensity was also investigated. Figure 5 shows the results of LIPS experiments on a $1.6 \times 10^{-3} M/M$ sample in which excitation intensity was varied over an order of magnitude while constant probe conditions were maintained. The dependence of the spectral shift ν_S on intensity is linear. In experiments with tripled YAG excitation, the spectral shifts were also found to depend linearly on excitation power. Spectral shifts between 0.1
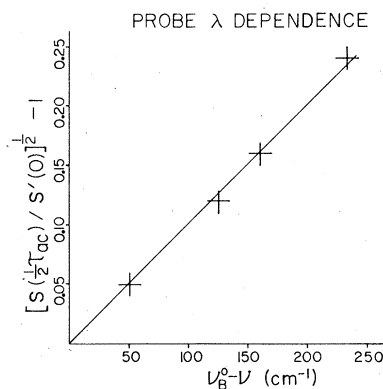

PROBE λ DEPENDENCE

FIG. 4. Probe wavelength dependence (with constant excitation conditions) of the amplitude of modulations in LIPS transient grating signal from a 2.9×10^{-5} M/M pentacene in p-terphenyl crystal. As the probe wavelength moves away from the pentacene absorption peak ($\nu_B^0 - \nu$ increases), the modulations in signal increase. The linear dependence shown is predicted by Eq. (15). The data give the same spectral shift, $\nu_S = 6.9$ cm^{-1}, for all wavelengths.
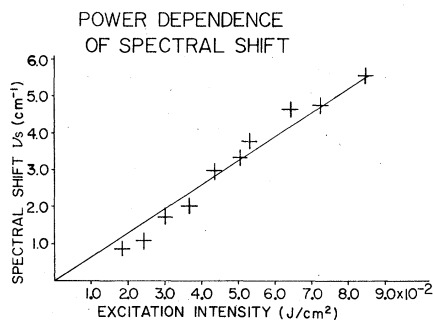
POWER DEPENDENCE
OF SPECTRAL SHIFT

FIG. 5. Excitation power dependence of spectral shift in a 1.6×10^{-3} M/M pentacene in p-terphenyl crystal. The linear dependence indicates that the strain amplitude is linear in excitation power and that the spectral shift is linear in the strain. Excitation wavelength is 532 nm.
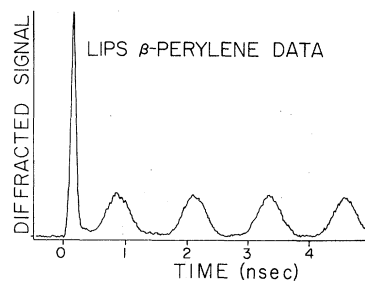

FIG. 6. LIPS transient grating data taken on a pure β-perylene crystal with 532-nm excitation and probe wavelengths. Acoustic waves propagate along the b crystallographic axis with wavelength $\Lambda = 3.5$ μm and speed $v_p = 2.8 \times 10^5$ cm/sec. Optical absorption at 532 nm is very weak, indicating that it is not the cause of the acoustic waves. After the initial spike, the signal is predominantly due to acoustic effects, indicating negligible excited-state concentration.

and 1.0 cm^{-1} were measured. The linear dependence was also observed in LIPS experiments performed on the pure molecular crystal system α-perylene.

The above results demonstrate that spectral shifts can be determined quantitatively and consistently under a variety of experimental conditions, and therefore the basic description of the influence of the acoustic disturbance on the transient grating observable is correct. We now will present experimental results which bear on the mechanism of production of the acoustic effects in the LIPS experiment. The results presented so far could be interpreted in terms of a previously proposed mechanism involving optical absorption into high-lying vibrational levels of S_1 and rapid radiationless relaxation producing heating with the grating spatial pattern. The linear intensity dependence of v_S would still be expected since absorption and therefore the density excursion would be linear in intensity.

The optical-absorption model can be tested by examining the spectral shift produced at any given excitation intensity as a function of the absorbing-species concentration. For a system like pentacene in p-terphenyl, the absorption

model predicts that the spectral shift should be sharply dependent on pentacene concentration. At higher concentration more excitation light is absorbed and the heat energy density and density excursion should be higher. Thus at higher concentration the spectral shift should be larger. Examination of a variety of samples with pentacene concentrations ranging over 2 orders of magnitude resulted in measurements of v_S which are independent of concentration. Experiments on three such samples are listed in Table I; 532-nm excitation was used. The table contains the measured values, as well as the values predicted by the absorption model for the lower concentrations once the necessary parameters are obtained from the highest concentration sample. Similar experiments performed with 355-nm excitation light showed the same type of results. Experiments on numerous samples of high, intermediate, and low concentration have consistently demonstrated that there is no dependence of v_S on pentacene concentration. These results clearly demonstrate that *heating through optical absorption is not responsible for driving the acoustic field.*

TABLE I. Concentration dependence of spectral shifts in pentacene in p-terphenyl. Experimental conditions were identical for all three crystals. The observed spectral shifts are independent of pentacene concentration. If optical absorption by pentacene were responsible for acoustic wave generation, the spectral shifts would decrease linearly with pentacene concentration as shown in the right column. This is clearly not observed.

Concentration (M/M)	Observed spectral shift v_S (cm^{-1})	v_S predicted by absorption model (cm^{-1})
1.6×10^{-3}	4.7	(4.7)
2.3×10^{-4}	4.0	0.68
2.9×10^{-5}	5.0	0.085

Additional evidence which argues against the absorption mechanism is provided by a number of other experiments. Modulations in TG signal due to spectral shifts were observed in experiments on samples in which the dye laser output, tuned to the red edge of the pentacene absorption profile, was used as the excitation source, and a 532-nm pulse was used as the probe. With the red excitation source the initially prepared state is vibrationally unexcited and very little heat could be deposited into the lattice due to absorption. Similarly, in α-perylene experiments the 532-nm excitation is far to the red of the $S_0 \rightarrow S_1$ absorption peak. In α-perylene, rapid excimer formation could lead to some heating. However, spectral shift modulations of the TG signal were also observed in LIPS experiments on β-perylene, a different crystalline form in which excimers are not produced.[17] Data from experiments on this sytem are shown in Fig. 6. Finally, phonon-induced modulations in the TG signal have been observed in samples of fluorene, a pure molecular crystal system whose $S_0 \rightarrow S_1$ absorption region is at 300 nm and which has only very weak two-photon absorption at 532 nm. In the β-perylene and fluorene experiments the probe was also 532 nm, and since this wavelength is only weakly absorbed, we believe that diffracted signal is mainly due to phonon-induced modulations in the real part of the index of refraction (a phase grating). Note that when there is no density excursion in the sample ($t = 0, 1, 2$, etc., acoustic cycles) there is almost no signal, indicating that excited-state concentration grating effects are absent. It is clear that acoustic wave generation occurs despite negligible optical absorption.

These experiments demonstrate that the phonon generation is not caused by heating through optical absorption. Direct coupling between the applied optical em field and the material acoustic field, as discussed in Sec. III B, must be responsible for the LIPS effect.

We wish to comment on the magnitude of the observed spectral shifts. In some experiments above, values of $\nu_s \sim 5$ cm^{-1} were measured. The maximum spectral shift in a LIPS experiment is $2\nu_s \approx 10$ cm^{-1}. Conventional density-dependent spectroscopy of organic molecular crystals, in which absorption spectra at high pressures (at least several kbar) are recorded, typically gives spectral shifts ranging from 20 to 80 cm^{-1} per kbar applied pressure.[3] This might suggest that pressures achieved in our experiments are quite high. However, the implications of high-pressure results for normal-density properties are unclear. First, compressibilities decrease with
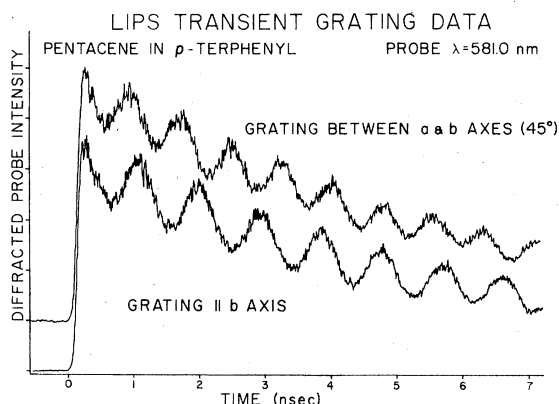

FIG. 7. LIPS transient grating data with acoustic waves propagating along various directions in 2.3×10^{-4} M/M pentacene in p-terphenyl. The amplitudes of modulation are roughly the same in the two traces, suggesting isotropic excited-state-phonon interactions in the ab plane. The acoustic wavelength in both experiments was $\Lambda = 2.44$ μm. The acoustic velocities were 2.57×10^5 cm/sec along the b axis and 3.08×10^5 cm/sec between axes.

increasing pressure so that as the pressure rises the density rises more and more slowly. A more fundamental problem is the fact that at high pressure one measures properties of a region of the crystalline potential energy surface far from the normal density equilibrium position. In fact the potential-energy surface itself may be severely altered, considering the large volume changes caused by these pressures. In p-terphenyl, for example, application of 10-kbar pressure causes a relative volume change of 10%.[18] Thus the spectral response to a density change at normal pressure could be very different from the response at high pressure. Once the theory connecting the applied em field to the acoustic response in LIPS experiments is completely detailed, calculation of the absolute strain in these "normal-pressure" experiments will become possible.

LIPS experiments with a variety of grating orientations were performed on pentacene in p-terphenyl crystals to investigate anisotropy in the excited-state phonon interactions. Data from these experiments are shown in Fig. 7. Grating alignments along the b axis, the a axis, and between the axes at numerous angles produced very little difference in the amplitude of the modulations of the TG signal. This suggests that the excited-state intermolecular interactions are rather isotropic in the ab plane. Since the variation in acoustic wave amplitudes at different grating orientations is not known, relative excited-state intermolecular interaction strengths can only be estimated. Nevertheless, it seems likely that
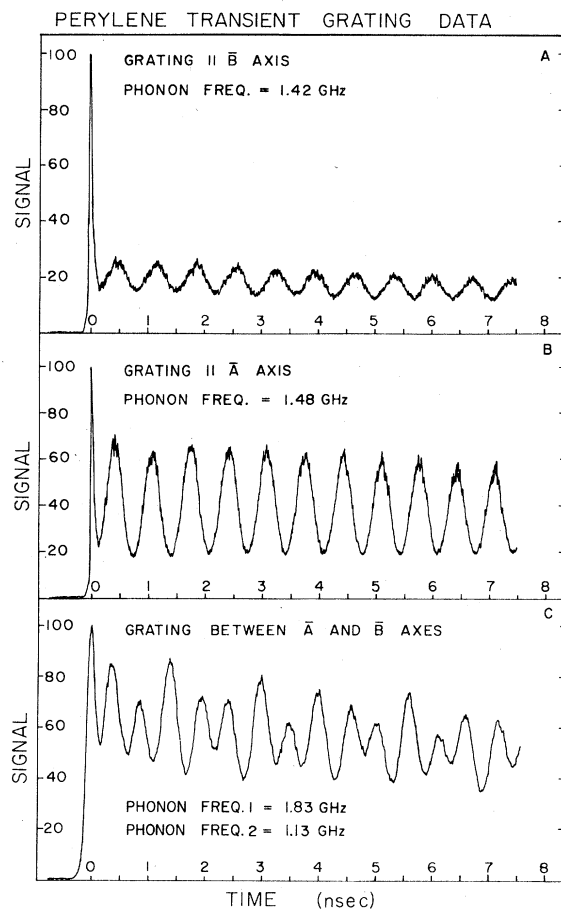
PERYLENE TRANSIENT GRATING DATA

FIG. 8. LIPS results for pure α-perylene. Acoustic wavelength is 1.73 μm in all cases. (a) Acoustic waves propagate along the b (symmetry) axis. Single-frequency modulation is observed. (b) Acoustic waves propagate along the a axis; single-frequency modulation is observed. (c) Waves propagate between a and b axes, in ab plane. Beating is due to generation of quasi-longitudinal and quasitransverse waves of identical wavelength but having different frequencies.

there is no strong anisotropy in the ab plane.

At any grating orientation, modulations of the TG signal occurred at a single frequency. This indicates that a single longitudinal wave was generated even though only the b axis is a symmetry-determined pure mode direction. The longitudinal wave velocity, measured in these experiments, was identical along the a and b axes (2.57×10^5 cm/sec) and fastest exactly between them (3.08×10^5 cm/sec), see Fig. 7. Apparently the acoustic properties of p-terphenyl are rather isotropic in the ab plane. These results are in sharp contrast to results obtained on α-perylene, displayed in Fig. 8. In this sytem only the a and b axes permit pure longitudinal waves, and at any other grating orientation beating between two
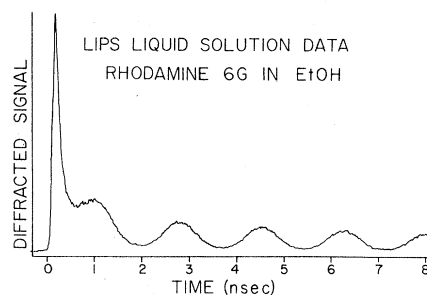

FIG. 9. LIPS transient grating data on a concentrated solution of Rhodamine 6G in ethanol. Excitation and probe wavelengths are 532 and 560 nm, respectively. The acoustic wavelength $\Lambda = 3.0$ μm and the speed of sound $v_p = 1.7 \times 10^5$ cm/sec. Diffracted signal due to an excited-state concentration grating vanishes with a concentration-dependent lifetime (Ref. 19).

waves of different frequencies is predicted and observed.[5]

The ab plane of p-terphenyl behaves almost like an isotropic medium such as a liquid. It is interesting to note that the considerations discussed in this paper also apply to liquids. Figure 9 presents experimental observation of the LIPS effect in a solution of Rhodamine 6G in ethanol.

VI. CONCLUDING REMARKS

In this paper we have presented a detailed description of the laser-induced-phonon effect. The nature of the acoustic disturbance was discussed and its effect on the transient grating observable was explicated. Measurements of the absolute size of electronic excited-state spectral shifts were reported. The LIPS effect was shown to be independent of optical absorption by the sample and a mechanism was proposed which involves the direct coupling of the em and acoustic fields. The effect was observed in a wide variety of samples. Thus the LIPS phenomenon is quite general and provides a method for the tunable generation of high-amplitude ultrasonic waves. These waves, which can be produced along selected crystallographic directions, were used to examine anisotropy in electronic excitation phonon interactions.

Here we have emphasized the application of LIPS to the study of excited-state intermolecular interactions. We now wish to suggest some other possible applications. As a method for convenient optical generation of tunable ultrasonic waves, the technique described here is clearly extremely useful. With YAG fundamental and harmonic frequencies, a tunable spectrum of acoustic frequencies to greater than 20 GHz can easily be achieved. The range can be extended with other

laser sources. Since optical absorption is not required for acoustic wave generation, a wide range of materials in the condensed phase should be amenable to this technique.

Amplitude and frequency modulation of light by light-generated phonons is possible with the LIPS technique. Note that the diffracted signal in the β-perylene experiments illustrated in Fig. 6 is almost 100% modulated by the LIPS effect. This phenomenon could have applications in optical communications.

LIPS measurements of acoustic properties have already been demonstrated. Elastic stiffness constants have been measured in several materials,[5] and acoustic loss properties could be easily measured. These types of measurements can provide information about phonon-phonon interactions, as well as having valuable applications in the measurements of physical properties of materials. The LIPS technique may be useful for nondestructive acoustic testing, acoustic holography, and acoustic microscopy. Optical generation of surface acoustic waves should be possible, and could lead to the develop-

ment of new experiments for the study of surfaces and interfaces.

Finally, the LIPS technique may be useful for studying condensed phase dynamics. For example, LIPS-generated ultrasonic waves could be used to dynamically drive a phase transition in the grating nulls which could be detected by Bragg diffraction if the nascent phase has different optical properties than the original phase. The ability of the material to undergo the density-wave-induced phase transition may depend on phonon frequency, e.g., at high frequancy, time may not permit the rearrangements necessary to change phase. This type of experiment could provide information about dynamics of phase transitions.

[1]M. Grover and R. Silbey, J. Chem. Phys. 52, 2009 (1970); A. S. Davydov, *Theory of Molecular Excitons* (Plenum, New York, 1971).

[2]Michael A. Collins and David P. Craig, Chem. Phys. 54, 305 (1981).

[3]P. F. Jones, J. Chem. Phys. 48, 5448 (1968); B. Y. Okamoto and H. G. Drickamer, *ibid.* 61, 2870 (1974); J. Donnini, J. Chim. Phys. 71, 1543 (1974).

[4]J. Merski and C. J. Eckhardt, J. Chem. Phys., in press.

[5]Keith A. Nelson and M. D. Fayer, J. Chem. Phys. 72, 5202 (1980).

[6]J. F. Nye, *Physical Properties of Crystals* (Oxford University, London, 1976); Donald F. Nelson, *Electric, Optic, and Acoustic Interactions in Dielectrics* (Wiley, New York, 1979).

[7]V. S. Starunov and I. L. Fabelinskii, Usp. Fiz. Nauk 98, 441 (1969) [Sov. Phys.—Usp. 12, 463 (1970)]; V. S. Starunov, Zh. Eksp. Teor. Fiz. 57 1012 (1969) [Sov. Phys.—JETP 30, 553 (1970)]; L. Landau and E. Lifshitz, *The Electrodynamics of Continuous Media* (Pergamon, London, 1960).

[8]J. R. Salcedo, A. E. Siegman, D. D. Dlott, and M. D.

Fayer, Phys. Rev. Lett. 41, 131 (1978).

[9]A. E. Siegman, J. Opt. Soc. Am. 67, 545 (1977).

[10]R. Collier, C. B. Burckhardt, and L. H. Lin, *Optical Holography* (Academic, New York, 1971).

[11]Max Born and Emil Wolf, *Principles of Optics*, 3rd ed. (Pergamon, Oxford, 1965).

[12]H. Kogelnik, Bell Syst. Tech. J. 48, 2909 (1969); T. Kubota, Opt. Acta 25, 1035 (1978).

[13]D. E. Caddes, C. F. Quate, and C. D. W. Wilkinson, Appl. Phys. Lett. 8, 309 (1966); A. Korpel, R. Adler, and B. Alpiner, *ibid.* 5, 86 (1964).

[14]Y. R. Shen and N. Bloembergen, Phys. Rev. 137, A1787 (1965); A. Yariv, IEEE J. Quantum Electron. QE-1, 28 (1965).

[15]Norman M. Kroll, J. Appl. Phys. 36, 34 (1965).

[16]R. G. Harrison, P. Y. Key, and V. I. Little, Proc. R. Soc. London A334, 193 (1973).

[17]J. Tanaka, T. Kishi, and M. Tanaka, Bull. Chem. Soc. Jpn. 47, 2376 (1974).

[18]S. N. Vaidya and G. C. Kennedy, J. Chem. Phys. 55, 987 (1971).

[19]D. R. Lutz, Keith A. Nelson, C. R. Gochanour, and M. D. Fayer, Chem. Phys., in press.